H1-11/96-504
November 28, 1996

Soft Interactions and Diffraction Phenomena

S.V. Levonian

LPNHE, Ecole Polytechnique, F-91128 Palaiseau, France
and LPI RAS, 117924 Moscow, Russia

`e-mail: levonian@polhp2.in2p3.fr`
`http://www-h1.desy.de/~levonian`

Plenary talk
given at the 28^{th} International Conference on High Energy Physics,
Warsaw, 25-31 July, 1996

Abstract

Until the mystery of confinement is understood from the first principles, so called *soft physics* remains an important area of research, providing valuable information on underlying dynamics of strong interactions at long distances. In this review an attempt is made to summarize recent experimental results on multiparticle production in e^+e^- annihilation and on diffraction at HERA.

SOFT INTERACTIONS AND DIFFRACTION PHENOMENA

S.V. LEVONIAN

LPNHE, Ecole Polytechnique, F-91128 Palaiseau, France
and LPI RAS, 117924 Moscow, Russia

Until the mystery of confinement is understood from the first principles, so called *soft physics* remains an important area of research, providing valuable information on underlying dynamics of strong interactions at long distances. In this short review an attempt is made to summarize recent experimental results on multiparticle production in e^+e^- annihilation and on diffraction at HERA.

1 Introduction

Contrary to a widely spread prejudice that soft physics at high energies is just a boring obstacle in the way of fast progress, I want to argue that it remains of a fundamental importance, providing us with new and valuable information about the underlying dynamics of strong interactions.

There are at least two basic reasons to study so called *soft processes* in particle physics. First of all, they represent the most fundamental challenge in QCD [1]. This is in contrast to the perturbative sector (pQCD), where the major theoretical problems are rather of a technical nature (to carry out difficult, but well defined calculations). Secondly, even if one is interested in precision pQCD tests, it is often difficult – if not impossible – to disentangle various non-perturbative effects. It is not only the unavoidable fragmentation phase, but also the presence of soft underlying events [2], originating from multiple parton-parton scattering, which can mask the properties of a hard subprocess. Therefore, until the nature of confinement is understood theoretically from first principles, experimental data which can shed additional light on the problem remain very important.

There exists a large variety of physics phenomena where non-perturbative QCD effects are essential. In this review three classes of such phenomena are discussed, for which new experimental results have been reported at the conference. These are: multiparticle production in e^+e^- annihilation, diffractive physics at HERA and the transition from soft to hard scattering in *ep* collisions. Theoretical aspects of diffraction in QCD will be discussed separately, by George Sterman in his plenary talk [3].

2 Multiparticle production

In this domain information about underlying production mechanisms is extracted by studying the correlations among produced particles.

A major difficulty in hadron-hadron collisions arises from the fact, that several non-perturbative effects get mixed here. Therefore, hard collisions are important to study the properties of hadronization, the only non-perturbative phase in the process. The details of the fragmentation at low scale, Q_0 can shed a light on the preconfinement stage (i.e. the dynamics between Q_0 and Λ_{QCD}) followed by the recombination of quarks and antiquarks into real hadrons.

e^+e^- collisions with their "clean QCD environment" provide the best laboratory for such kind of measurements. A typical strategy here is to calculate analytically the partonic cascade down to a scale Q_0 and then apply a phenomenological hypothesis, like e.g. local parton-hadron duality [4], to end up with observable hadron distributions which can be confronted with experimental data.

When the basic properties of parton-to-hadron fragmentation are established, one can go back to a difficult case of hadron-hadron collisions, to learn more about non-perturbative dynamics there.

2.1 Quark and Gluon Jet Properties

One of the specific QCD predictions is a difference between the properties of quark and gluon initiated jets. This effect is due to the different relative probabilities for a gluon or a quark to radiate an additional gluon, given by the Casimir factors $C_A = 3$ and $C_F = 4/3$ respectively. Experiments [5] confirm, at least at the qualitative level, that gluon jets are “richer”: they have a softer and significantly broader fragmentation function and they are characterized by larger average multiplicity, as compared to quark jets. To study this effect the experiments at LEP use high statistics (few 10^6 hadronic Z_0 decays) and their excellent ability to tag jet flavour (with a typical purity of $\sim 80 \div 90\%$) in the clean QCD environment of e^+e^- annihilation.

Especially interesting is to study the ratio

$$r \equiv \langle n \rangle_{gluon} / \langle n \rangle_{quark}$$

for which analytical QCD calculations exist. From the theoretical side, the progress over the last two decades in computing the ratio r resulted in decreasing its value from $r = C_A/C_F = 9/4$ in leading order QCD [6] to $r = 1.84 \pm 0.02$ in higher order QCD, taking into account recoil effect in the soft gluon emission [7]. Experiments however found lower values, concentrated around $r \approx 1.2$.

A word of caution is in order here. Whereas the theoretical calculations refer to the parton multiplicities originating from $q\bar{q}$ or gg states, experiments measure charged particles, applying in addition specific jet algorithms to select three jet events $e^+e^- \rightarrow q\bar{q}g$ as a source of gluon jets. Hence the experimental results depend upon the jet algorithm chosen [5].

It was demonstrated [7,8] with the help of Monte Carlo simulations, that hadronization, when taken into account, brings the theoretical value closer to those measured experimentally. In order to eliminate a mismatch between the theoretical and experimental definitions of a gluon jet, a new method was proposed [8], based upon rare topologies of $e^+e^- \rightarrow q\bar{q}g$ events, in which both quark jets appear in the same hemisphere of an event and hence are balanced by the gluon. In this case the multiplicity $\langle n \rangle_{gluon}$ can be determined without applying a jet algorithm, just by counting the particles in the ‘gluon hemisphere’.

New results presented at this conference [9], are based on yet higher statistics as well as improved particle identification and flavor tagging technique. DELPHI has measured $r = 1.16 \pm 0.01$ at $\langle E \rangle = 24$ GeV and $r = 1.28 \pm 0.02$ at $\langle E \rangle = 30$ GeV, using a natural mixture of all quark flavours in their sample ($q = udscb$).

OPAL, motivated by the fact that massless quarks are used in theoretical calculations, made

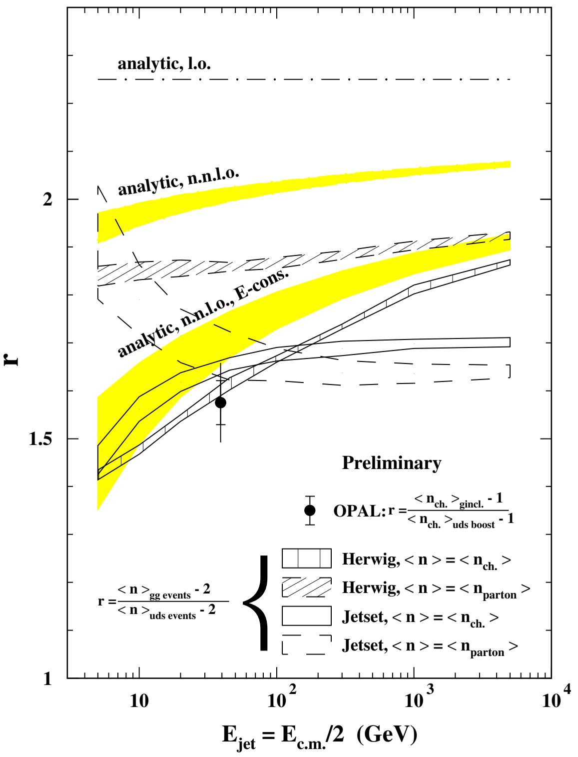

Figure 1: QCD analytic and Monte Carlo predictions for the ratio of the mean particle multiplicity between gluon and quark jets as a function of jet energy, in comparison to the OPAL measurement for 39 GeV jets [10].

a step further by separating light and heavy quarks and has shown, that

$$\langle n_{ch} \rangle (uds) < \langle n_{ch} \rangle (b) < \langle n_{ch} \rangle (g),$$

leading to different values of $r = 1.09 \pm 0.03$ for ($q = b$) and $r = 1.39 \pm 0.05$ (for $q = uds$), at $\langle E \rangle = 24$ GeV.

In yet another OPAL analysis [10] a full use of all available statistics was necessary in order to exploit the new method of Gary [8], described above. Only 221 out of $3.04 \cdot 10^6$ events were selected for the final ‘gluon-sample’. As a result, a value of

$$r = 1.575 \pm 0.046_{stat} \pm 0.069_{syst}$$

was obtained, for the average energy of $\langle E \rangle = 39$ GeV. As one can see from Fig. 1 this value is already in a very good agreement with both analytic calculations and Monte Carlo predictions.[a]

[a] There was also new CLEO result [11], presented at the

2.2 Multiplicity Distributions

Multiplicity distributions (MD), i.e. a set of probabilities, P_n to produce n-particle final state, are natural and most widely used characteristics of multiparticle production. The state of the art in this field can be found in recent reviews [12,13]. In this section two questions are briefly discussed:

- do we understand the basic properties of MD at least in hard scattering, taking as an example the process $e^+e^- \to Z_0 \to hadrons$?
- is there an analogy between MD in hard (e^+e^-) and predominantly soft (hh) collisions?

Apart from well known average multiplicity, $\langle n \rangle$, and dispersion, D, other observables are used in modern analyses of MD [12]: factorial (F_q) and cumulant (K_q) moments of rank q, and, since recently, their ratio, $H_q = K_q/F_q$. These quantities are helpful in the mathematical description of branching processes, and they are widely used in various scientific fields to describe the properties of cascade phenomena[14]. It has been shown[15] that the ratio H_q is not only sensitive to the shape of MD, but also can be calculated in higher-order pQCD.

Phenomenologically, the best description of the MD in e^+e^- annihilation is provided by the negative binomial (NBD) or the log-normal (LND) distributions [12]. Even they however fail to reproduce all the details observed in the data. In particular, experimental data show two interesting features [16,17]:

1) a pronounced shoulder in MD in the range of intermediate multiplicities and

2) a quasi-oscillatory behavior of the ratio H_q as a function of rank q.

In the paper [18] presented to this conference, authors attempted to find a common origin of both aforementioned effects. They have shown (see Fig. 2 and Fig. 3) that good quantitative description of the data can be obtained by a superposition of two NBD's with the relative proportion given by the ratio of 2-jet to multi-jet events as defined in the same experiments. It was also demonstrated that the truncation effect ($n_{ch} < n_{max}$) in experimentally measured MD cannot be neglected.

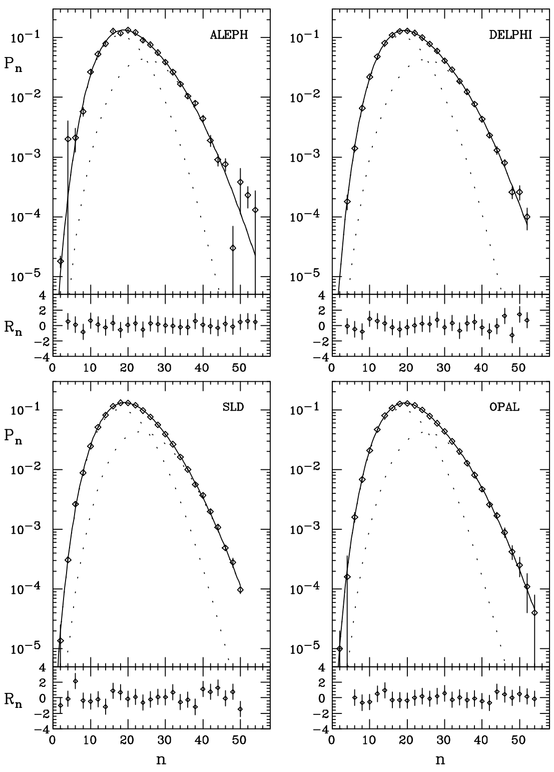

Figure 2: Charged particle multiplicity distributions, P_n, measured at the Z_0 peak, as compared to the superposition of two NBD contributions (solid curves), which are also shown separately (dotted curves). The residuals, R_n, are shown underneath each of the distributions.

Thus, the shape of MD in e^+e^- annihilation can be understood in terms of the multi-jet event topology, predicted by pQCD.

Let us now turn to the "dirty" world of hh-collisions. Here the bulk of the cross section is due to soft, low p_t processes, and hence pQCD approach is not fully justified. Surprisingly, we find nevertheless, that both discussed features of MD are well familiar in hh experiments as well [19,20].

As we have seen, an essential ingredient for a successful description of the data is a *two-component* structure of MD. In hard collisions (e^+e^-) it could be identified with two- and multi-jet events. What is the origin of these components in predominantly soft hh processes? Looking further back in history, we do find a good candidate. It was shown that the Dual Parton Model

conference: $r = 1.04 \pm 0.02(\text{stat}) \pm 0.04(\text{syst})$, obtained for jet energies less than 7 GeV. For the correct interpretation however one has to treat threshold effects properly. It seems there is simply no phase space available to develop a fat partonic cascade at this low energy.

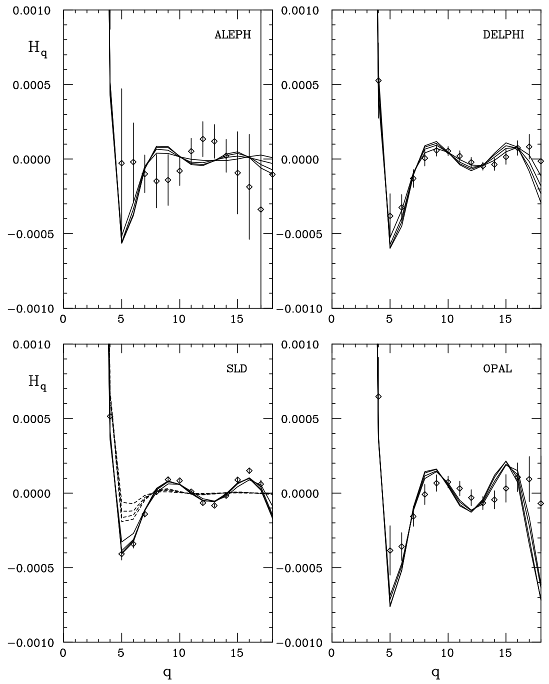

Figure 3: The ratio H_q as a function of the rank, q. The data are compared to the superposition of two NBD, weighted according to the relative proportion of 2- and multi-jet events, as measured in each of the shown experiments. The difference between the dashed and the solid lines at SLD plot shows the effect of the truncation of MD.

(DPM) [21], based on Reggeon field theory [22], is able to reproduce the shape of KNO-distributions and to describe two-particle correlations in high energy pp- and $\bar{p}p$ -collisions. In the framwork of DPM, multi-pomeron exchanges, which are necessary to unitarize the hadron-hadron scattering amplitude, naturally lead to the different event topologies, consisting of 1-, 2-, ... Pomeron strings.

It would be very interesting to see whether the oscillations of H_q are also reproduced by DPM.

3 Diffraction and Physics of Pomeron

Another large area where soft physics plays the dominant rôle is diffraction. The basic properties of diffractive processes – cross sections exponentially falling with four momentum transfer squared, t, predominantly low mass final states, $M^2 \ll s$, large rapidity intervals between the diffractively produced hadronic systems, etc. – have been established already in the 60's and 70's in hadron-hadron scattering experiments. These properties are typical for soft, peripheral interactions, and they found a best and most natural explanation in a framework of Regge approach [23,24]. A number of comprehensive review articles [25–27] nicely summarise the experimental status in this field and the interpretation of the data in terms of Regge theory.

Since the advent of the parton model and then QCD a main emphasis was shifted to *hard processes*, leaving for diffraction only a little attention. A spike of interest was caused by the observation of jets in $\bar{p}p$ diffractive final states [28], following the pioneering proposal by Ingelman and Schlein [29], who invented a concept of the Pomeron structure function. A real "Renaissance" however was triggered by early HERA data [30] on the proton structure function, F_2 at low x, and the observation of large rapidity gap events in deep inelastic ep scattering [31]. Only then it was clearly realized, that diffraction and low x physics at HERA are closely related subjects with high potential to provide a completely new insight into non-perturbative QCD effects, as well as to bridge the soft (Regge) and hard (pQCD) domains.

3.1 Total Cross Sections and Pomeron

In Regge theory the asymptotic behavior of the energy dependences of total, elastic and diffractive dissociation cross sections is defined by the properties of the leading vacuum (Pomeranchuk) trajectory:

$$\alpha_{I\!P}(t) = 1 + \lambda + \alpha'_{I\!P} t \qquad (1)$$

with the intercept $\alpha_{I\!P}(0) \equiv \Delta = 1 + \lambda$. As has been demonstrated by Donnachie and Landshoff [32], the energy dependence of *any* total hadronic cross section σ_{ab} can be described in a very economical form

$$\sigma_{ab} = X_{ab} \cdot s^{\lambda} + Y_{ab} \cdot s^{-\eta} \qquad (2)$$

with universal powers

$$\lambda \approx 0.0808, \quad \eta \approx 0.4525 \qquad (3)$$

being independent of the type of colliding particles a and b (Fig. 4). This simple Regge inspired parametrization, when applied to photoproduction, successfully predicted $\sigma_{\gamma p}$ at HERA energies. At this conference new data have been presented by the L3 Collaboration [33] on total gamma-gamma cross sections at small virtualities $\langle Q^2 \rangle =$

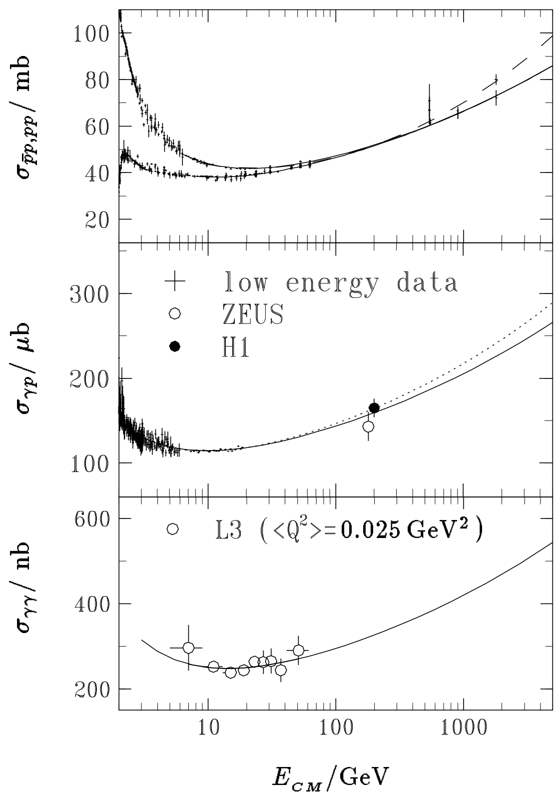

Figure 4: Energy dependence of the total $pp, \bar{p}p, \gamma p$ and $\gamma\gamma$ cross sections. The curves represent the DL parametrization (2) with $\lambda = 0.0808$ (solid), $\lambda = 0.112$ (dashed) and $\lambda = 0.088$ (dotted).

0.025 GeV^2. The data have been extracted from e^+e^- collisions at $\sqrt{s} = 130, 136$ and 140 GeV, recently collected at LEP on its way to LEP-200. As one can see in Fig. 4 these data are also consistent with the parametrization (2). The dashed and the dotted curves on Fig. 4 demonstrate the energy dependence (2) with $\lambda = 0.112$ and $\lambda = 0.088$ respectively, obtained separately from the best description of the Tevatron data [34] and of photoproduction data including HERA measurements[35] into the fit. It should be stressed however, that the original result (3) remains a good *global* fit of all total hadronic cross sections, leading to a very attractive concept of a *universal Pomeron.*

In all so far discussed reactions soft, long distance physics represents the dominant contribution. Therefore, the value of $\Delta \approx 1.08$ is often referred to as the intercept of the 'soft' Pomeron. In case of deep inelastic scattering (DIS) where it is natural to expect hard processes to dominate, a much steeper rise was observed of $\sigma_{tot}(\gamma^* p)$ with energy W, (or, equivalently, a rise of F_2 with decreasing Bjorken x) which can be approximated by a power low $(W^2)^\lambda$ with $\lambda \approx 0.2 \div 0.4$ depending on the virtuality Q^2 of the photon [36]. At the beginning it was tempting to explain this fast rise as a manifestation of perturbative BFKL Pomeron[37], which in leading logarithmic approximation (LLA) corresponds to

$$\lambda_{BFKL} = \frac{4N_c \ln 2}{\pi}\alpha_s \approx 0.4 \div 0.5 \qquad (4)$$

This value of λ_{BFKL}, as was pointed out by the authors themselves [38], should not be seen uncritically, since next-to-leading order corrections may significantly change the result of LLA calculation. Therefore, more realistic and cautious expectation for the intercept of the 'hard' Pomeron (sometimes also referred to as the *QCD Pomeron*) is $\lambda \geq 0.2 \div 0.3$.

Reaching this stage, an innocent reader may immediately conclude:

$$0 < \lambda_{soft} < \lambda_{hard} < \lambda_{BFKL} \leq 0.5$$

and wonder, how many pomerons are there after all? Moreover, whatever the exact value of λ is, eq. (2) will sooner or later violate the Froissart bound.

The variety of the opinions can be summarized in the following way. First of all, everybody agrees, that unitarity corrections to one-pomeron exchange are necessary, although different technical schemes were proposed for the unitarization procedure: multi-pomeron exchanges [39], eikonalization of the scattering amplitude[40], or the combination of both [41]. Thus, the intercept of the 'bare' Pomeron may be significantly different from the 'effective' intercept measured in the experiments, depending on how large unitarity corrections to a single-pomeron exchange amplitude are. At this point the opinions (models) start to diverge:

1) At presently available energies unitarity corrections are negligible, and the universal 'bare' Pomeron has an intercept of $\Delta \approx 1.08$. These models are in fact ruled out by F_2 measurements at HERA.

2) The universal (i.e. the same in hadron-hadron and in DIS reactions) 'bare' Pomeron has an intercept of $\Delta \approx 1.25$. The effect of screening

(unitarity) corrections depends on both the energy and a typical hard scale involved. The value of $\Delta_{eff} = 1.08$ observed in hadronic reactions is thus a result of large corrections, whereas in DIS the corrections become small with increasing Q^2, and hence the 'bare' Pomeron is seen.

3) 'Bare' Pomeron $\equiv$ BFKL Pomeron, but screening corrections are so large that the effective power λ becomes smaller even in the DIS case.

4) There is no Pomeron whatsoever in DIS. The rise of F_2 at small x can be equivalently well described by the conventional DGLAP [42] evolution equations, while the rapidity gap events in DIS may be due to various mechanisms [43], which do not need the concept of Pomeron.

Further, more illuminating discussion about the 'soft' and 'hard' Pomeron can be found elsewhere [44]. From our point of view, there is only one Pomeron (and in that sense it is universal), which however receives contributions from both non-perturbative and perturbative exchanges. Depending on the experimental conditions, either soft, or hard component will dominate, thus leading to the different values of λ observed. Screening corrections may additionally reduce the value of the 'effective' intercept.

As already was mentioned (for details see Ref. [3,36]), F_2 measurement alone is too inclusive to conclude unambiguously on BFKL dynamics. Therefore, dedicated measurements of diffractive processes are necessary to decide whether or not 'hard' Pomeron is seen at HERA. We now turn directly to this topic.

3.2 Large Rapidity Gap Events and Diffraction

Experimentally, diffractive processes at HERA are studied by looking for so called *Large Rapidity Gap* events (Fig. 5), which are naturally expected, and are not exponentially suppressed, in the case of colourless exchange between the proton and the virtual photon. Defining as usual $Q^2 = -q^2$ and $W^2 = (q+p)^2$, where q and p denote the 4-vectors of the virtual photon and the proton respectively, further relevant kinematic variables can be introduced:

$$t = (p-Y)^2, \quad x_{I\!P} = \frac{Q^2 + M_x^2}{Q^2 + W^2}, \quad \beta = \frac{Q^2}{Q^2 + M_x^2}.$$

Note, that despite the suggestive names (e.g.

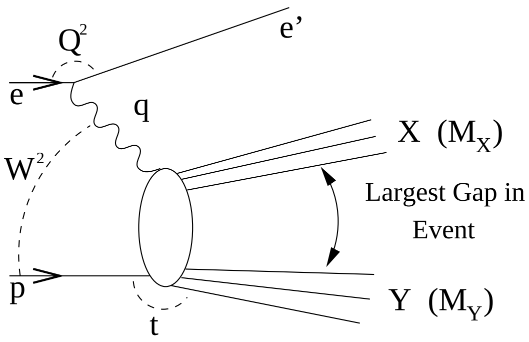

Figure 5: Generic diagram for a rapidity gap event in *ep* scattering.

$x_{I\!P}$) the described experimental definition is completely general. A cross section measured at different values of the aforementioned kinematical variables is free of any assumptions on the nature of contributing processes. It is only when interpreting the results in terms of diffractive dissociation that one has to select a kinematical range where the Pomeron exchange dominates (small $x_{I\!P} \leq 0.05$) and to take into account possible remaining non-diffractive contributions.

The H1 and ZEUS experiments use the capabilities of their forward detectors to either identify the leading baryonic system Y as a proton or a neutron, or to restrict its mass, $M_Y < 1.6 \div 2$ GeV, if the system Y is not directly observed. This guarantees the gap between the hadronic systems X and Y to be larger than 3 to 4 units in rapidity. Furthermore, the specifically asymmetric kinematics of HERA, due to very different proton and lepton beam energies, ensures a uniquely high detector acceptance for the diffractively produced hadronic system X. This enables precision measurements of the diffractive dissociation of virtual photon at HERA. Finally, high resolving power (Q^2) of the virtual photon allows for the first time in high energy physics the partonic substructure of the exchanged object in diffraction to be probed.

3.3 Soft Diffractive Processes

A special interest to soft diffractive processes is related to the expectation to see an effect of unitarity corrections to the diffractive cross sections at presently available energies. Indeed, since a Pumplin limit [45], $\sigma_{el}/\sigma_{tot} \leq \frac{1}{2}$, is violated signifi-

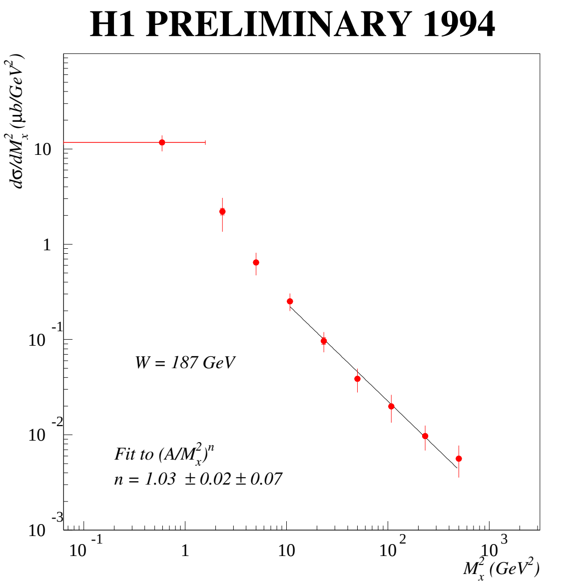

Figure 6: The differential cross section, $d\sigma/dM_X^2$ for the process $\gamma p \to XY$ in the kinematic region $M_Y < 1.6$ GeV and $|t| < 1$ GeV^2. A fit is shown for $10.8 < M_X^2 < 500$ GeV^2.

cantly earlier than the Froissart bound [46], $\sigma_{tot} < c\ln^2 s$, one expects unitarity corrections to a single pomeron exchange to become more important in diffractive processes compared to the total cross section. First experimental evidence of this has been reported for $\bar{p}p$ collisions at the Tevatron [47].

It is well known in Regge phenomenology that the information about the Pomeron intercept can be extracted not only from the energy dependences of the total and diffractive cross sections, but also from the diffractive mass distributions. Moreover, in the context of eikonal models [40] the differential cross section $d\sigma^D/dM_X^2 \propto (M^2)^{-(\Delta+2\alpha'_{I\!P}t)}$ is not affected by screening corrections. Hence a 'bare' Pomeron intercept is expected to be seen. Thus comparing the values of Δ extracted from the diffractive mass distributions with those obtained from the energy dependence of the cross sections may provide important information about screening corrections in soft diffractive processes.

At this conference two HERA experiments have presented first preliminary data on inclusive diffractive photoproduction at comparable energies of $\langle W_{\gamma p}\rangle = 187$ GeV (H1 [48]) and $\langle W_{\gamma p}\rangle = 200$ GeV (ZEUS [49]). Triple Regge analyses of the diffractive mass spectra in the reaction $\gamma p \to M_X p$ (see Fig. 6), after correcting for the unmeasured t-dependences, yield the intercept values, entirely consistent with the 'soft' Pomeron:

$$\begin{aligned} \text{H1:}\quad & \Delta = 1.11 \pm 0.02_{stat} \pm 0.07_{syst}, \\ \text{ZEUS:}\quad & \Delta = 1.14 \pm 0.04_{stat} \pm 0.08_{syst}. \end{aligned}$$

Yet the data and their precision are insufficient for any firm conclusion about the importance of screening corrections at HERA energies.

3.4 Hard Diffraction at HERA

First direct information about the partonic structure of the Pomeron can be extracted from the inclusive measurements in diffractive DIS:

$$\frac{\mathrm{d}^3\sigma^D}{\mathrm{d}\beta dQ^2 \mathrm{d}x_{I\!P}} = \frac{4\pi\alpha^2}{\beta Q^4}(1-y+\frac{y^2}{2})F_2^{D(3)}(\beta,Q^2,x_{I\!P}), \tag{5}$$

where $y = Q^2/(sx)$ is the inelasticity parameter. New data on the differential cross section (5) have been presented by ZEUS [50] and H1 [51]. High statistics, based on 2 pb^{-1} of 1994 data, enables H1 to perform QCD analysis of the diffractive structure function $F_2^{D(3)}$ which resulted in the parton distributions, shown in Fig. 7. As one can see more than 80% of the momentum in the diffractive exchange is carried by gluons. Important technical details of this interesting analysis are described in Ref. [51].

Such a 'gluon dominated Pomeron' leads to definite predictions about the properties of the hadronic final states in DIS diffraction, which can be confronted with experimental data. For example, as illustrated by Fig. 8, more energy flow, bigger $\langle p_t\rangle$ and lower thrust values in the $\gamma^* I\!P$ centre of mass system are expected in case of a gluon dominated exchanged object, as compared to a quark dominated one. A significant difference is also expected in the production rates of charm and of high E_t jets.

These predictions are indeed supported by the data, as shown for example in Fig. 9 and as discussed in more details elsewhere [52].

The partonic structure of the Pomeron, as measured in DIS, is also consistent, at least qualitatively, with diffractive *photoproduction* of high E_t jets. This is illustrated by Fig. 10(a,b) where ZEUS data [54] are seen to prefer a hard gluon density in the Pomeron. Another interesting observation in this analysis, shown in Fig. 10c, is that

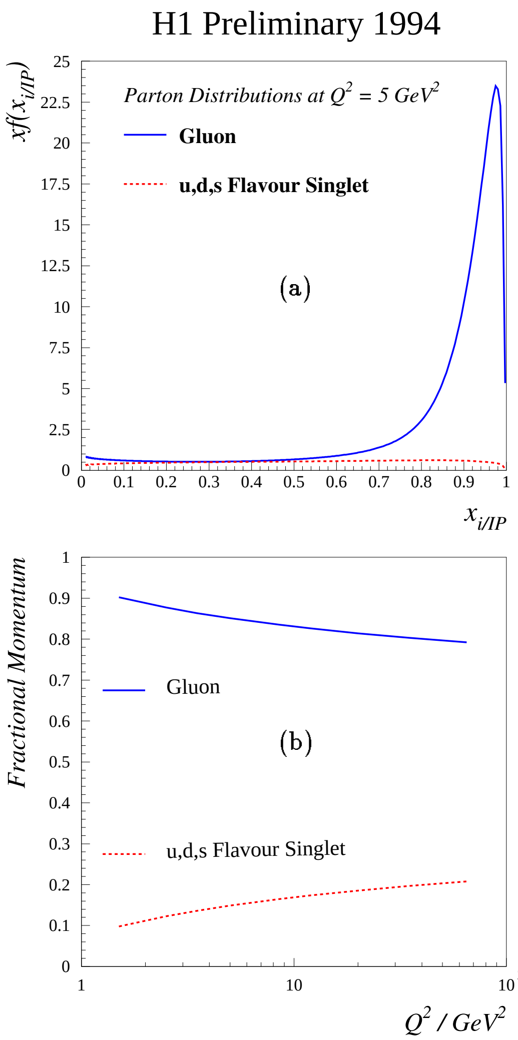

Figure 7: (a) Partonic content of the Pomeron at the starting scale, $Q^2 = 5$ GeV^2 resulted from QCD fit [51] of the diffractive structure function $F_2^{D(3)}$; (b) fraction of the total momentum in diffractive exchange carried by quarks and by gluons, as a function of Q^2.

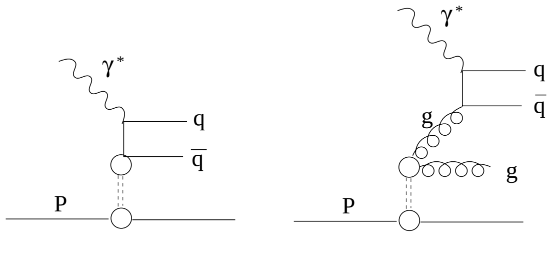

Figure 8: Feynman diagrams for quark and gluon initiated processes in diffractive DIS.

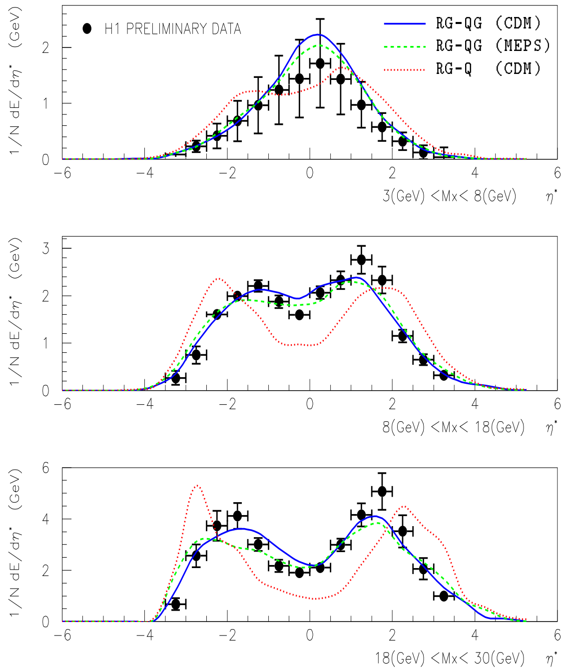

Figure 9: Energy flows in the $\gamma^* I\!P$ centre of mass system in three bins of M_X, as measured in the H1 detector [52]. The data are compared to RAPGAP [53] Monte Carlo predictions, using either pure quark (Q), or gluon dominated (QG) parton densities in the Pomeron.

a sizable proportion of diffractive hard photoproduction is produced via the so called *resolved* photon contribution, in which only a fraction of the photon momentum, x_γ participates in the hard subprocess.

The H1 measurement [51] of the Pomeron intercept,

$$\Delta = 1.18 \pm 0.02_{stat} \pm 0.04_{syst},$$

extracted from the $x_{I\!P}$-dependence of the cross section (5), is in agreement with the result of a similar ZEUS analysis [50] and is somewhat larger, than the intercept of the 'soft' Pomeron.

When interpreting these results it should be remembered, that in a fully inclusive case, integrating over all possible diffractive final states, both high p_t (short distance) and low p_t (long distance) partonic configurations contribute, and it is not a priori clear which ones will dominate. There are arguments [55] for low p_t physics to prevail even in the case of DIS diffraction. Therefore, to isolate a possible contribution from the 'hard' Pomeron, it

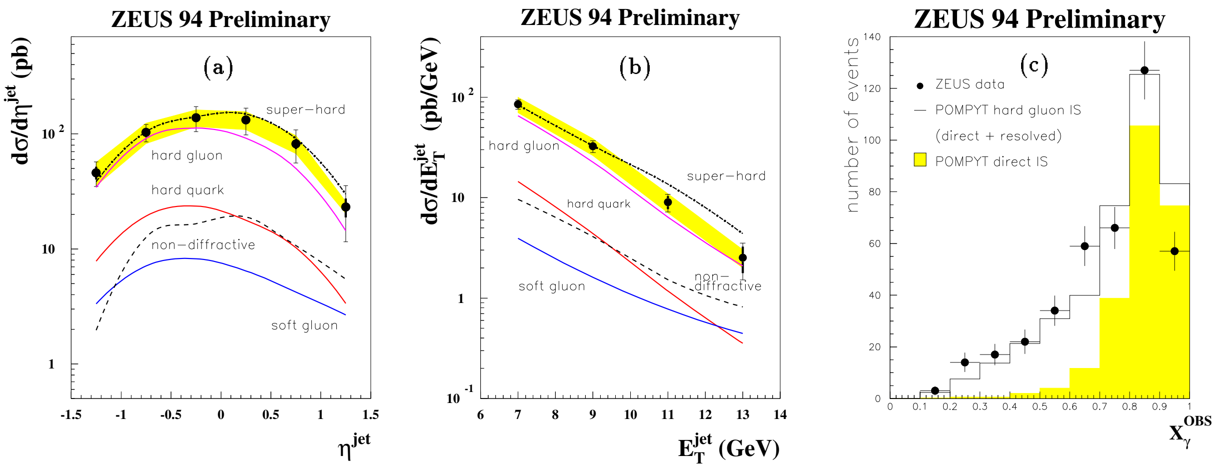

Figure 10: Dijet cross sections in diffractive photoproduction at HERA, as measured in the ZEUS detector[54].

is necessary to select specific final states for which hard scale physics processes control the cross section (heavy quarks [56,57], vector mesons produced by longitudinally polarized virtual photons[58], high E_t jets etc.) Statistically adequate data samples for such kind of analyses, permitting quantitative comparisons with pQCD calculations and capable for discriminating between various models, require higher luminosities at HERA and yet improved detector capabilities, which are both in progress.

3.5 Photoproduction of Vector Mesons

Exclusive vector meson production in *ep* collisions, being sensitive both to the intercept Δ and to the slope $\alpha'_{I\!P}$ of the leading Regge trajectory (1), provides yet another possibility to study the properties of the Pomeron at HERA. A great attention to this area was attracted after it was realized, that in many cases pQCD is applicable allowing the cross sections to be analytically calculated [56,58,59]. It was shown, that the evaluated cross sections are proportional to the square of the gluon density in the target, thus providing a very sensitive measure of the gluon distribution in the nucleon. In this section a brief overview is given of the experimental status of elastic photoproduction of vector mesons at high energies. New data on electroproduction of vector mesons at high Q^2 are discussed elsewhere [36].

A whole bunch of fresh results [63,64,65] on elastic and diffractive photoproduction of light mesons (ρ^0, ω) has been reported at this conference by the ZEUS Collaboration. For the first time at HERA t-distributions were directly measured by exploiting the Leading Proton Spectrometer of ZEUS. The measurements of the slope b of the differential cross section, $d\sigma(\gamma p \to \rho^0 p)/dt = Ae^{bt}$ at different energies are compiled in Fig. 11a. It is seen, that the shrinkage of the 'diffractive cone' is well described by the parameters of the 'soft' Pomeron. For comparison, the behavior of the slope b as a function of Q^2 (Fig. 11b) and W (Fig. 11c) are also shown in case of elastic electroproduction of ρ^0. Remembering that the slope b reflects a typical interaction radius: $b \propto (R_p^2 + r_\perp^2)$, one can conclude that the radius $r_\perp$ increases with energy W and decreases with virtuality Q^2, in qualitative agreement with expectations. In this somewhat simplified picture, when $r_\perp$ becomes much smaller than the size of the proton, R_p, the slope b asymptotically tends to a constant value. This corresponds to $\alpha'_{I\!P} \approx 0$ for the 'hard' Pomeron. More precise data on t-distributions in elastic electroproduction of vector mesons are required in order to measure the evolution of $\alpha'_{I\!P}$ with Q^2 at HERA.

New measurements of elastic J/ψ photoproduction at HERA [66] are compared in Fig. 12 to low energy data and to the model prediction [56], based on pQCD calculations and using two different parametrizations for the proton structure function. One can see, that the rate of J/ψ production grows with energy significantly faster, as compared to the Regge inspired expectation, $\sigma_{el} \propto W^{4\lambda}$, based on the 'soft' Pomeron ($\lambda \approx 0.08$). On

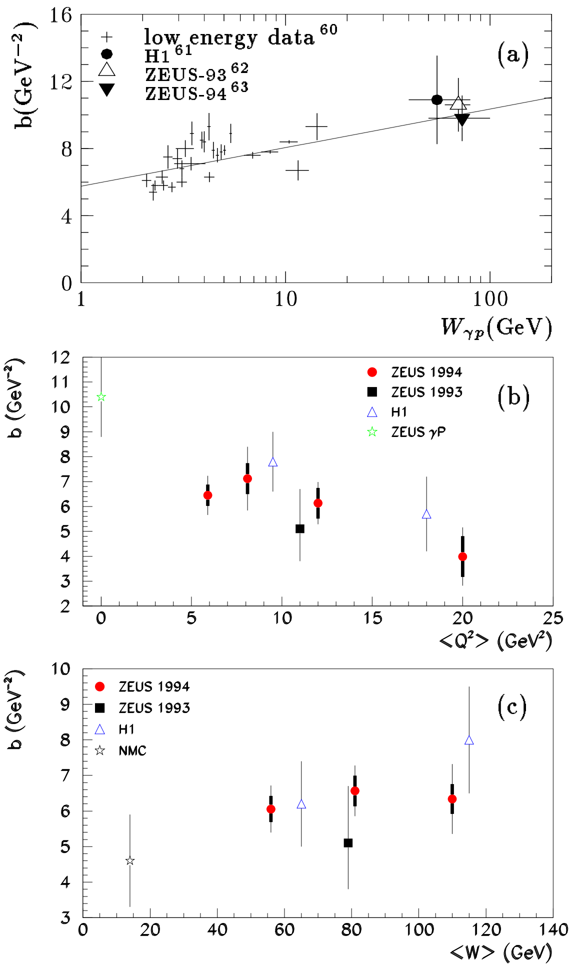

Figure 11: Energy dependence of the elastic slope in (a) photo- and (c) electroproduction. The full line shows Regge parametrization $b = b_0 + 2\alpha'_{\mathbb{P}} \ln W^2_{\gamma p}$ with $b_0 = 5.75$ and $\alpha'_{\mathbb{P}} = 0.25$; (b) Q^2 dependence of the slope of elastic electroproduction of ρ^0 mesons at HERA.

the contrary, the measured cross section is in good agreement with pQCD model, showing in addition the predicted sensitivity to the gluon density in the proton. One should mention, that another model [67], based upon Reggeon field theory with Q^2 dependent unitarity corrections, also gives a very good description of the data [68].

The energy dependences of the total and elastic (ρ, ω, ϕ and J/ψ) photoproduction cross sections are compiled in Fig. 13. A clear difference in the steepness indicates the transition from the 'soft' to 'hard' Pomeron caused by the large mass of the charm quark, which defines a hard scale in case of J/ψ production.

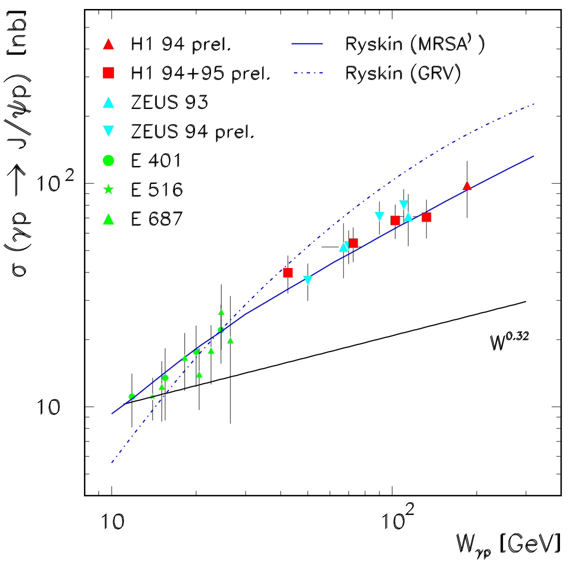

Figure 12: Energy dependence of elastic J/ψ photoproduction. The line $W^{0.32}$ indicates the prediction, based on 'soft' Pomeron.

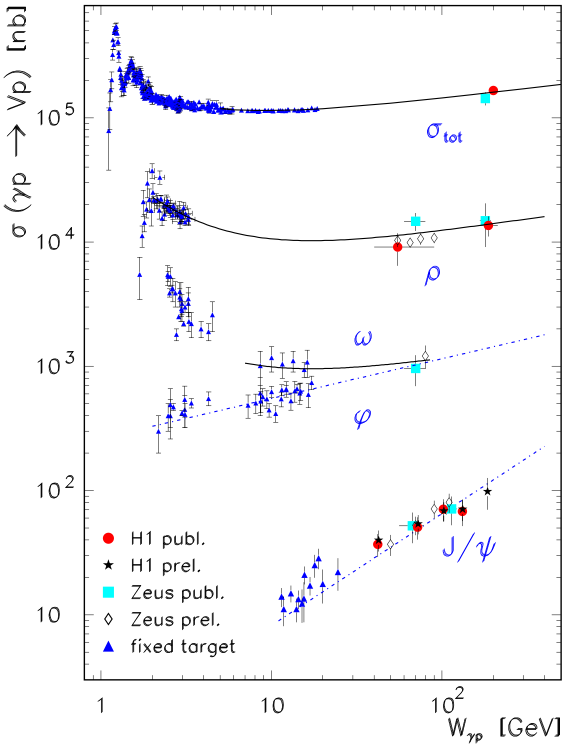

Figure 13: Total γp and exclusive vector meson photoproduction cross sections.

3.6 Concluding Remarks

To summarize, both soft and hard diffractive processes have been observed at HERA, in real and virtual photon-proton collisions. The data reveal characteristic features of either a *soft* (non-perturbative), or a *hard* (perturbative) Pomeron, depending on the value of the typical scale involved, in qualitative agreement with theoretical expectations. The properties of diffractively produced final states in photoproduction as well as in the DIS regime are consistent with 'leading' gluon component in the Pomeron.

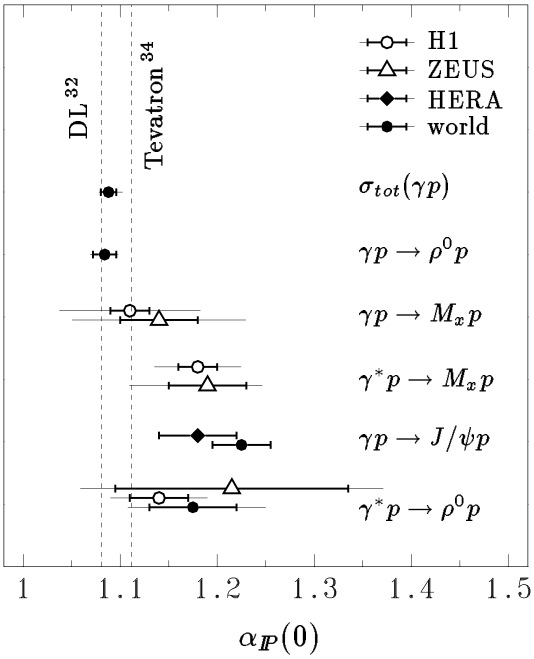

Figure 14: Summary on the Pomeron intercept measurement at HERA. Thick inner bars represent statistical errors, while the total (thin) bars correspond to statistical and systematic errors added in quadrature. Dashed lines show the values obtained from the combined fit of the total hadronic cross sections [32] and from the Tevatron data [34].

A summary of the Pomeron intercept measurements at HERA is presented in Fig. 14. Although no evidence is found for the naive leading order BFKL Pomeron (4), the data clearly show the departure from the 'soft' Pomeron towards larger values of $\alpha_{I\!P}(0)$, whenever a *hard scale* is present. More precise data coming from new HERA run are expected to further clarify this intriguing situation.

4 From Soft to Hard Physics

One of the 'goldplated' fields of research at HERA is to study how the properties of photon and the dynamics of its interaction with protons evolve with Q^2, by comparing real and virtual photon-proton interactions in identical experimental conditions. Interesting information can be extracted from both inclusive measurements and more detailed properties of the hadronic final states. A review of recent ideas in modelling the transition from photoproduction to DIS regime can be found elsewhere [69].

New measurements of the proton structure function F_2 at HERA, presented at this conference [70], have demonstrated that perturbative QCD successfully describes the data down to surprisingly low $Q^2 \simeq 2$ GeV^2. The transition between 'soft' ($\lambda \approx 0.08$) and 'hard' ($\lambda \geq 0.2$) regimes occurs, at HERA energies, at $Q^2 \approx 1$ GeV^2.

Another way to study similarities and differences between photoproduction and DIS has been presented by the H1 Collaboration [71]. The idea of the analysis, as illustrated in Fig. 15, is to use high p_t charged particles as a measure of a typical scale in γp process, which can be varied in a similar way as a scale Q^2 in DIS.

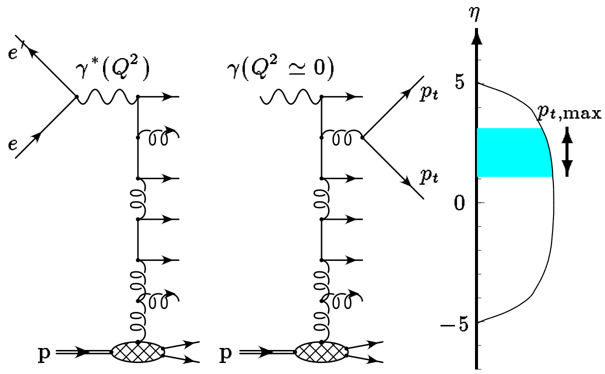

Figure 15: Schematic diagrams for DIS event and photoproduction event with high p_t particles in the final state. The sketch on the right side illustrates an inclusive charged particle pseudorapidity distribution in γp centre of mass system, with the range used to search for high p_t tracks in the H1 detector.

Good detector acceptance and high resolution of p_t measurement, together with large statistics of γp events, allow a continuous coverage of both soft and hard scattering domains. Simi-

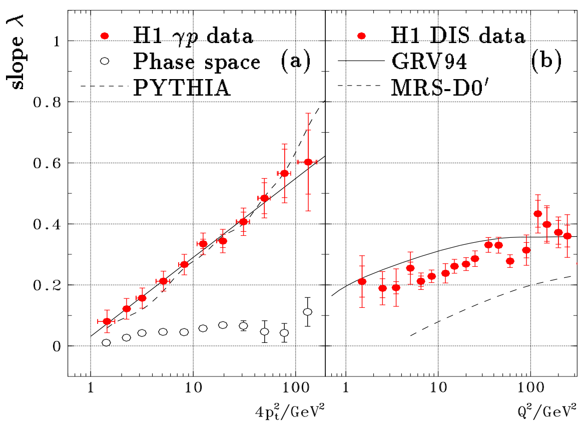

Figure 16: The scale dependence of the slope λ in photoproduction (a) and DIS (b). The full line in (a) represents the result of a linear fit $\lambda_{\gamma p} = C \cdot \ln(4p_t^2) + \lambda_0$ to the data, with $C = 0.112 \pm 0.007$ and $\lambda_0 = 0.031 \pm 0.014$. The PYTHIA prediction is based on Monte Carlo version [72] which includes both pQCD for the hard scattering process and a Regge inspired soft interaction component.

lar to $\sigma_{\gamma^* p}(W, Q^2) \propto W^{2\lambda(Q^2)}$ in DIS, the photoproduction cross section was parametrized as $\sigma_{\gamma p}(W, p^2_{t,\max}) \propto W^{2\lambda(p^2_{t,\max})}$ with the scale defined by the maximum p_t charged particle in the photon fragmentation region. The results of this analysis are shown in Fig. 16. One can see a clear similarity in the evolutions of the W dependence of γp and $\gamma^* p$ cross sections with increasing scales ($4p^2_{t,\max}$ and Q^2 respectively). Another interesting observation is that the transition from soft to hard regimes proceeds in both cases smoothly.

This similarity can be qualitatively understood both in terms of pQCD and in terms of a Regge approach. In perturbative QCD the effect of more steeply rising cross sections with increasing hard scale can be readily explained by leading order partonic scattering contributions [73,74], while in Reggeon Field Theory (RFT) it is a consequence of the reduction of unitarity corrections to one-pomeron exchange [67,75].

It is informative to compare also the properties of the hadronic final states in photoproduction and DIS. As was explained in Section 3.2 experimental conditions at HERA allow the measurements in the central rapidity plateau in the $\gamma^* p$ centre of mass system, and are especially favorable to study the photon fragmentation region.

From simple, but very general arguments [76] the central region is expected to depend only on the total energy, but not on the type of colliding particles. This was verified in hadron-hadron collisions. All the difference between real and virtual photon-proton interactions is expected to be seen in the photon fragmentation region: at high Q^2 the situation should resemble the e^+e^- annihilation case, whereas final states produced by real photons are expected to be similar to those in hadron-hadron collisions. In particular, one expects transverse energy flow, particle multiplicity and $\langle p_t \rangle$ to grow with Q^2.

First analysis of HERA data along this line [77], in which energy flow was compared in γp and DIS reactions, confirmed the picture. At this conference new preliminary analysis has been reported [78] in which charged particle spectra in pseudorapidity, $dN_{ch}/d\eta$, are studied in two data samples: $Q^2 \approx 0$ and $\langle Q^2 \rangle = 15$ GeV^2, at $\langle W \rangle = 190$ GeV.

In Fig. 17 the data from non-diffractive $\bar{p}p$ [79], γp and $\gamma^* p$ interactions are compared. Surprisingly, we discover, that the difference between similar 'soft' reactions ($\bar{p}p$ and γp) is even bigger than between γp and DIS samples. This means that the whole difference in charged particle multiplicity between photoproduction and DIS in the photon fragmentation region is related entirely to the different proportion of diffractive events in the two reactions. This somewhat unexpected result remains to be understood and explained.

H1 PRELIMINARY

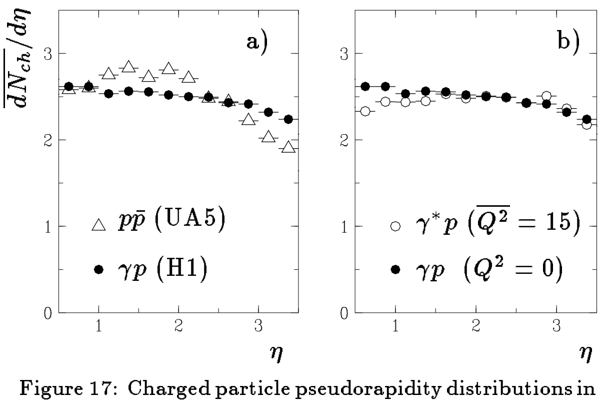

Figure 17: Charged particle pseudorapidity distributions in non-diffractive interactions of $\bar{p}p$ at $E_{cm} = 200$ GeV and γp, $\gamma^* p$ at $W = 190$ GeV.

Apart from the already discussed motivation, it is interesting to test a remarkable property of RFT, that the unitarity correction contributions cancel in inclusive particle cross sections in the

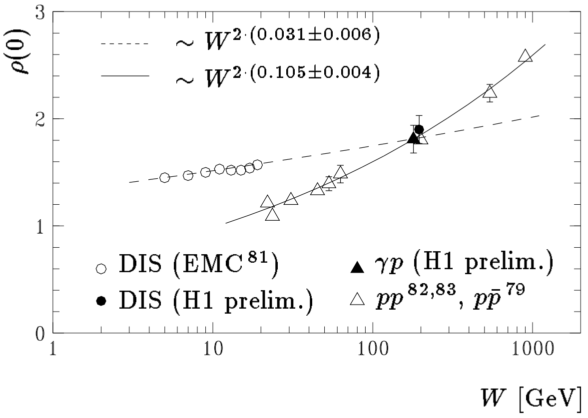

Figure 18: Energy dependence of the charged particle density in the central rapidity region in different reactions.

central rapidity region. This is a direct consequence of AGK cutting rules[80], which relate multi-pomeron exchange diagrams of RFT to particle production. Hence, within this framework the behavior of

$$\left.\frac{d\sigma_{ch}}{d\eta}\right|_{\eta\approx 0} \stackrel{\rm AGK}{=} \sigma^{(1)} \left.\frac{dN^{(1)}_{ch}}{d\eta}\right|_{\eta\approx 0} \qquad (6)$$

is predicted to be universal in all types of high energy reactions and is defined by the properties of the 'bare' one-pomeron exchange, denoted in eq. (6) by superscript $^{(1)}$.

Fig. 18 shows the energy dependence of the charged particle density

$$\rho(0) = \frac{1}{\sigma_{tot}} \frac{d\sigma_{ch}}{d\eta}$$

in the central rapidity region in DIS, photoproduction and hp interactions. It is observed that the energy dependence of DIS data is significantly weaker. This is in agreement with prediction (6), and is explained by the difference in the energy dependence of $\sigma_{tot}(\gamma p/hp)$ and $\sigma_{tot}(\gamma^* p)$.

To further test the validity of RFT predictions, it would be interesting to compare the shapes of MD and two-particle correlation functions for which differences are expected between photoproduction and DIS.

5 Summary

Soft processes represent an essential part of high energy physics. An ultimate goal here is to gain analytic control over confinement and thus to complete QCD as a theory of strong interactions. The task is difficult, but worth the effort. All experimental facilities are important, providing complementary information in this field of research.

Recent experimental data have demonstrated that perturbative QCD works extremely well down to surprisingly low scales, both in the description of time-like partonic cascades in e^+e^- annihilation and space-like cascades in deep inelastic scattering.[b]

Interesting qualitative similarities have been observed between hard processes (e^+e^- annihilation, DIS) and those which are predominantly driven by soft physics (hh collisions, γp scattering). This can provide a good basis for understanding the relations between Regge theory and QCD, as well as underlying dynamics in the transition region between the two.

One of the best opportunities to investigate an interplay between soft and hard physics is offered by diffractive deep inelastic scattering. For the first time we have a powerful facility for detailed study of the partonic content of diffractive exchange. Yet more precise data from HERA, together with improving detector capabilities promise that an interesting life in this field will continue, challenging the theorists and providing new insights into the properties of the Pomeron both in perturbative and non-perturbative regimes.

Acknowledgements

It is a pleasure to thank Professor A.K. Wroblewski and the Organizing Committee for the kind invitation to give a review talk at this conference. I am also grateful to my colleagues from H1, ZEUS, OPAL, DELPHI and L3 for providing me with their data and for many useful discussions. Special thanks go to John Dainton for taking a critical look at the manuscript.

[b] In that respect, an interesting analogy has been noted [84] at this conference, between the energy dependence of the charged particle multiplicity in e^+e^- annihilation and the rise of F_2 at low x at HERA. The theorists are invited to judge whether this is just a lucky chance, or a natural feature of pQCD dynamics. In any case, an amazing consequence is that one could predict low x behavior of the F_2 by measuring $\langle n_{ch}\rangle_{e^+e^-}(s)$ and vise versa!

References

1. D.J. Gross, *Toward a String Theory of QCD*, lecture given at SUSY school (1994)
2. G. Knies, *J. Phys. G: Nucl. Part. Phys.* **19**, 1523 (1993); T. Sjöstrand, *J. Phys. G: Nucl. Part. Phys.* **22**, 709 (1996).
3. G. Sterman, *Hard scattering, low x and diffraction – theoretical aspects*, these proceedings.
4. G. Marchesini, L. Trentadue and G. Veneziano, *Nucl. Phys.* **B181** (1981) 335; Ya.I. Azimov, Yu.L. Dokshitzer, V.A. Khoze and S.I. Troyan, *Z. Phys.* **C27** (1985) 65; *idem*, *Z. Phys.* **C31** (1986) 213; L. Van Hove and A. Giovannini, *Acta. Phys. Pol.* **B19** (1988) 917.
5. For recent reviews see: J.W. Gary, Proc.of the XXV Int.Symp. on Multiparticle Dynamics, Stará Lesná, Sep.12-16 (1995); I.G. Knowles et al., *Physics at LEP 2*, Vol. 2, CERN 96-01 (1996)
6. S.J. Brodsky and J. Gunion, *Phys. Rev. Lett.* **37** (1976) 402; K.Konishi, A. Ukawa and G. Veneziano, *Phys. Lett.* **B78** (1978) 243.
7. I.M. Dremin and R.C. Hwa, *Phys. Lett.* **B324** (1994) 477; I.M. Dremin and V.A. Nechitailo *Mod. Phys. Lett.* **A9** (1994) 1471.
8. J.W. Gary, *Phys. Rev.* **D49** (1994) 4503.
9. DELPHI Collab., contributed paper 02-012; OPAL Collab., contributed paper 02-013; ALEPH Collab., contributed paper 04-065.
10. OPAL Collab., contributed paper 02-014.
11. CLEO Collab., contributed paper 04-050.
12. E.A. De Wolf, I.M. Dremin and W. Kittel, *Phys. Rep.* **270** (1996) 1.
13. S. Lupia, PhD Thesis, (Turin U.) RX-1575 (1995)
14. A. Bialas and R. Peschanski, *Nucl. Phys.* **B273** (1986) 703.
15. I.M. Dremin et al., *Mod. Phys. Lett.* **A8** (1993) 2747.
16. DELPHI Collab., P. Abreu et al., *Z. Phys.* **C52** (1991) 271; OPAL Collab., P.D. Acton et al., *Z. Phys.* **C53** (1992) 539; ALEPH Collab., D. Buskulic et al., *Z. Phys.* **C69** (1995) 15.
17. SLD Collab., K. Abe et al., *Phys. Lett.* **B371** (1996) 149.
18. A. Giovannini, S. Lupia and R. Ugoccioni, *Phys. Lett.* **B374** (1996) 231. *idem.*, contributed paper 02-006.
19. UA5 Collab., R.E. Ansorge et al., *Z. Phys.* **C43** (1989) 357.
20. I.M. Dremin et al., *Phys. Lett.* **B336** (1994) 119.
21. A. Capella and J. Tran Thanh Van, *Z. Phys.* **C10** (1981) 249; A.B. Kaidalov, *Phys. Lett.* **B116** (1982) 459; P. Aurenche et al., *Z. Phys.* **C23** (1984) 67; *idem., Z. Phys.* **C26** (1984) 279; F. Bopp et al., *Z. Phys.* **C51** (1991) 99; A. Capella et al., *Phys. Rep.* **236** (1994) 225.
22. V.N. Gribov, *Sov. Phys. JETP* **26** (1968) 414.
23. T. Regge, *Nuovo Cimento* **14** (1959) 951; T. Regge, *Nuovo Cimento* **18** (1960) 947; G. Chew and S. Frautchi, *Phys. Rev. Lett.* **7** (1961) 394; G. Chew, S. Frautchi and S. Mandelstam, *Phys. Rev.* **126** (1962) 1202.
24. P.D.B. Collins, *An Introduction to Regge Theory and High-Energy Physics*, 445p., Cambridge (1977)
25. A.B. Kaidalov, *Phys. Rep.* **50** (1979) 157.
26. G. Alberi and G. Goggi, *Phys. Rep.* **74** (1981) 1.
27. K. Goulianos, *Phys. Rep.* **101** (1983) 169.
28. UA8 Collab., R. Borino et al., *Phys. Lett.* **B211** (1988) 239; UA8 Collab., A. Brandt et al., *Phys. Lett.* **B297** (1992) 417.
29. G. Ingelman and P. Schlein, *Phys. Lett.* **B152** (1985) 256.
30. H1 Collab., I. Abt et al., *Nucl. Phys.* **B407** (1993) 515; ZEUS Collab., M. Derrick et al., *Phys. Lett.* **B316** (1993) 412; H1 Collab., T.Ahmed et al., *Nucl. Phys.* **B439** (1995) 471; ZEUS Collab., M. Derrick et al., *Z. Phys.* **C65** (1995) 379.
31. ZEUS Collab., M. Derrick et al., *Phys. Lett.* **B315** (1993) 481; H1 Collab., T.Ahmed et al., *Nucl. Phys.* **B429** (1994) 477.
32. A. Donnachie and P.V. Landshoff, *Phys. Lett.* **B296** (1992) 227.
33. L3 Collab., contributed paper 02-036.
34. CDF Collab., F.Abe at al., *Phys. Rev.* **D50** (1994) 5550.
35. ZEUS Collab., M. Derrick et al., *Z. Phys.* **C63** (1994) 391; H1 Collab., S. Aid et al., *Z. Phys.* **C69** (1995) 27.

36. H. Abramowicz, *Tests of QCD at low x*, these proceedings.
37. E.A. Kuraev, L.N. Lipatov and V.S. Fadin, *Sov. Phys. JETP* **45** (1977) 199; Y.Y. Balitski and L.N. Lipatov, *Sov. J. Nucl. Phys.* **28** (1978) 822.
38. V.S. Fadin and L.N. Lipatov, preprint DESY 96-020 (1996); V. Del Duca, preprint DESY 95-249 (1995); L.N. Lipatov, preprint DESY 96-132 (1996)
39. A. Capella, J. Kaplan and J. Tran Thanh Van, *Nucl. Phys.* **B105** (1976) 333; A. Capella and A.B. Kaidalov, *Nucl. Phys.* **B111** (1976) 477; A.B. Kaidalov, L.A. Ponomarev and K.A. Ter-Martirosyan, *Sov. J. Nucl. Phys.* **44** (1986) 468.
40. E. Gotsman, E. Levin and U. Maor, *Z. Phys.* **C57** (1993) 667; *idem, Phys. Rev.* **D49** (1994) 4321; U. Maor, Proc. of the Topical Conf. *Hard Diffractive Processes*, Eilat (1996) p.72.
41. E.S. Martynov and B.V. Struminsky, *Phys. Rev.* **D53** (1996) 1018.
42. V.N. Gribov and L.N. Lipatov, *Sov. J. Nucl. Phys.* **15** (1972) 438; G. Altarelli and G. Parisi, *Nucl. Phys.* **B126** (1977) 298; Yu.L. Dokshitzer, *Sov. Phys. JETP* **46** (1977) 641.
43. W. Buchmüller and A. Hebeker, *Phys. Lett.* **B355** (1995) 573; G. Ingelman, A. Edin and J. Rathsman, *Phys. Lett.* **B366** (1996) 371.
44. J. Bartels in Proc. *DIS and QCD*, Eds. J.-F. Laporte and Y. Sirois, Paris (1995) p.105.
45. J. Pumplin, *Phys. Rev.* **D8** (1973) 2899.
46. M. Froissart, *Phys. Rev.* **123** (1961) 1053.
47. CDF collab., F. Abe et al., *Phys. Rev.* **D50** (1994) 5535.
48. H1 Collab., contributed paper 02-067.
49. ZEUS Collab., contributed paper 02-048.
50. ZEUS Collab., contributed paper 02-026.
51. H1 Collab., J.P. Phillips, these proceedings; H1 Collab., contributed paper 02-061.
52. H1 Collab., J.P. Phillips, these proceedings; H1 Collab., contributed papers 02-060, 02-062, 02-068.
53. H. Jung, *Comp. Phys. Comm.* **86** (1995) 147.
54. ZEUS Collab., contributed paper 02-039.
55. J.D. Bjorken, preprint SLAC-PUB-7096 (1996)
56. M.G. Ryskin, *Z. Phys.* **C37** (1993) 89.
57. E.M. Levin et al., preprint DTP/96/50 (1996)
58. L. Frankfurt and M. Strikman, *DIS and QCD*, Eds. J.-F. Laporte and Y. Sirois, Paris (1995) p.159; E. Gotsman, E. Levin, U. Maor, preprint TAUP 233896/96 (1996)
59. S.J. Brodsky et al., *Phys. Rev.* **D50** (1994) 3134; J. Nemchik et al., preprint DFTT 71/95 (1996)
60. G. McClellan et al., *Phys. Rev. Lett.* **22** (1969) 374; C. Berger et al., *Phys. Lett.* **B39** (1972) 659; Y. Eisenberg et al., *Phys. Rev.* **D5** (1972) 15; J. Ballam et al., *Phys. Rev.* **D5** (1972) 545; G. Gladding et al., *Phys. Rev.* **D8** (1973) 3721; W. Struczinski et al., *Nucl. Phys.* **B108** (1976) 45; D. Aston et al., *Nucl. Phys.* **B209** (1982) 56; W.D. Shambroom et al., *Phys. Rev.* **D26** (1982) 1.
61. H1 Collab., S. Aid et al., *Nucl. Phys.* **B463** (1996) 3.
62. ZEUS Collab., M. Derrick et al., *Z. Phys.* **C69** (1995) 39.
63. ZEUS Collab., Derrick et al., preprint DESY 96-183 (1996)
64. ZEUS Collab., contributed paper 02-051.
65. ZEUS Collab., contributed paper 02-049.
66. ZEUS Collab., contributed paper 02-047; H1 Collab., contributed paper 02-085.
67. A. Capella et al., *Phys. Lett.* **B337** (1994) 358.
68. L.P.A. Haakman, A. Kaidalov and J.H. Hoch, *Phys. Lett.* **B365** (1996) 411.
69. A. Levy, preprint TAUP 2349-96 (1996); B. Badelek and J. Kwiecinski, *Rev. Mod. Phys.*, to be published.
70. ZEUS Collab., contributed paper 02-025; H1 Collab., contributed paper 02-070.
71. J. Gayler, these proceedings; H1 Collab., S. Aid et al., preprint DESY 96-224 (1996).
72. T. Sjöstrand, CERN-TH-6488 (1992), *Comp. Phys. Comm.* **82** (1994) 74.
73. D.Cline, F. Halzen and J. Luthe, *Phys. Rev. Lett.* **31** (1973) 493.
74. W. Buchmüller and D. Haidt, preprint DESY 96-061 (1996)
75. A.L. Ayala, M.B. Gay Ducati and E.M. Levin, ANL-HEP-PR-96-52 (1996)
76. J.D. Bjorken and J. Kogut, *Phys. Rev.* **D8** (1973) 1341; J.D. Bjorken, SLAC summer school, SLAC-167 (1973) 1.

77. H1 Collab., S. Aid et al., *Phys. Lett.* **B358** (1995) 412.
78. K. Müller, these proceedings.
79. UA5 Collab. G.J.Alner, et al., *Z. Phys.* **C33** (1986) 1.
80. V.A. Abramovskii, V.N. Gribov and O.V. Kancheli, *Sov. J. Nucl. Phys.* **18** (1974) 308.
81. EMC Collab., M.Arneodo et al., *Z. Phys.* **C35** (1987) 335.
82. W.Thomé et al., *Nucl. Phys.* **B129** (1977) 365.
83. NA22 Collab., M.Adamus et al., *Z. Phys.* **C39** (1988) 311.
84. A. De Roeck and E.A. De Wolf, contributed paper 02-093 and preprint DESY 96-143 (1996)